Study on optimal design and vibration characteristics of diaphragm spring based on Genetic algorithm

F J Wang[1,3,4]*, Y Z Cui[1,3,4], F X Xu[1,3,4], S Bai[1], P C Xia[1], J F Wang[2]

1. Qiqihar University, Qiqihar, 161006, China

2. Qiqihar Heavy CNC Equipment Co., Ltd., Qiqihar, 161006, China

3. Heilongjiang Province Collaborative Innovation Center for Intelligent Manufacturing Equipment Industrialization, Qiqihar, 161006, China

4. The Engineering Technology Research Center for Precision Manufacturing Equipment and Industrial Perception of Heilongjiang Province, Qiqihar, 161006, China

ABSTRACT

The parameters of diaphragm spring are optimized and the dimensional parameters in this design are determined with careful derivation. The global optimization feature of the genetic algorithm is used to optimize the diaphragm spring and compared with the damping effect of the standard algorithms. The results show that the optimization design can significantly reduce the force and realize vibration control of the clutch when the design requirements are met. Due to the large error in calculating the vibration characteristics of diaphragm spring by the commonly used A-L method, the finite element method is used to study the influence of the separation finger structure on the load-deflection characteristics of diaphragm spring. To this end, three different window shapes of diaphragm springs are verified in real-life measurements, and the effective pressure test data for three types of diaphragm springs (type A, type B and type C) are selected. Finally, the load displacement of the peak and valley is obtained by summing their averages under loading and unloading of each diaphragm spring model. Moreover, a new method for calculating the vibration characteristics is obtained by introducing the genetic algorithms into the optimal design of diaphragm springs. Compared the A-L method, the finite element method and the proposed method with the measured data, it is verified that the proposed method has high accuracy in calculating the vibration characteristics of diaphragm springs.

1. INTRODUCTION

One of the main devices of the automotive transmission system is the clutch, which is mainly used to cut off and transmit the engine torque to enable it to start normally [1]. The clutch plays a vital role in the entire automotive transmission system. Its performance will directly affect the braking, service cost and service life of the vehicle. High performance and excellent technical support of the clutch are necessary to ensure optimal handling of vehicles.

*Corresponding Author: wangy213@yeah.net

The designed clutch can accurately transmit the torque emitted by the engine during the normal driving process of the vehicle, which is conductive overload protection. The diaphragm spring clutch has a small moment of inertia, which can protect the vehicle from damage that caused by the unevenness of the shifting gear [2]. To improve the performance of the clutch, it is necessary to optimize the diaphragm spring, and use a method to calculate near-precision fast. The genetic algorithm (GA) has the advantages of high accuracy and fast speed and is not easy to fall into local optimal solution, so that it is easier to obtain a more accurate global optimal solution [3-4].

Diaphragm spring is made of spring steel plate and is divided into two parts: disc springs and separating fingers. It is widely used in automotive clutches because of its non-linear characteristics and many other excellent properties. The A-L equation proposed by Almen and Laszlo is currently used as the theoretical basis for the preliminary analysis of diaphragm springs [5]. The A-L method is an approximate formula for calculating disc springs, but with theoretical errors in derivation. The load-deflection curve calculated by the finite element method was closer to the measured curve than the A-L method [6-8]. To calculate the vibration characteristic curves of diaphragm springs, the influence of the separation finger structure is analyzed, and the objective functions are established to optimize the mathematical model of diaphragm springs. In this way, a new method for calculating the vibration characteristics of diaphragm springs is presented by integrating the genetic algorithm into the optimal design, and its accuracy is verified by the test.

2. DETERMINATION OF DIAPHRAGM SPRING PARAMETERS

The structure of diaphragm spring can be seen as consisting of a disc spring part and a separation finger [9]. The main parameters are shown in Fig. 1. R is the big end radius; r is the small end radius; H is the cone height; h is the thickness of the spring piece; δ_1 is the width of the small end groove; δ_2 is the width of window slot; δ_3 is the contact width between the separation finger and the inner diameter; r_0 is the inner longitude of the small end of the diaphragm spring; r_e is the inner radius of the window; r_f is the separation radius of the bearing, and n is the segregation index order.

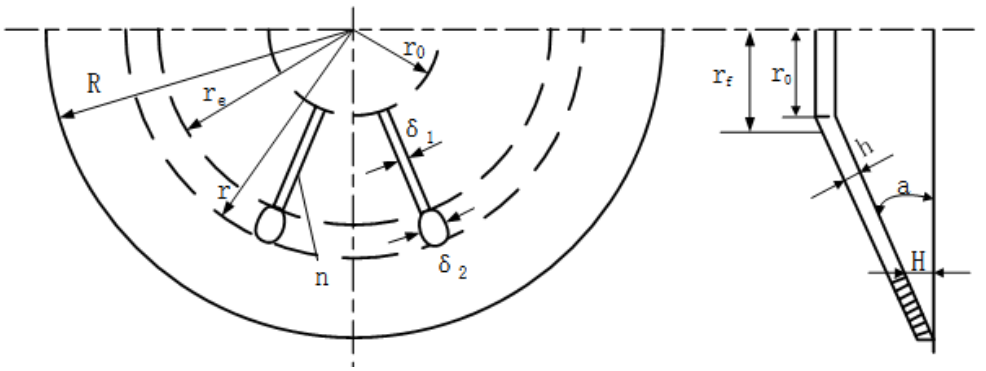

(a) Rectangular window hole

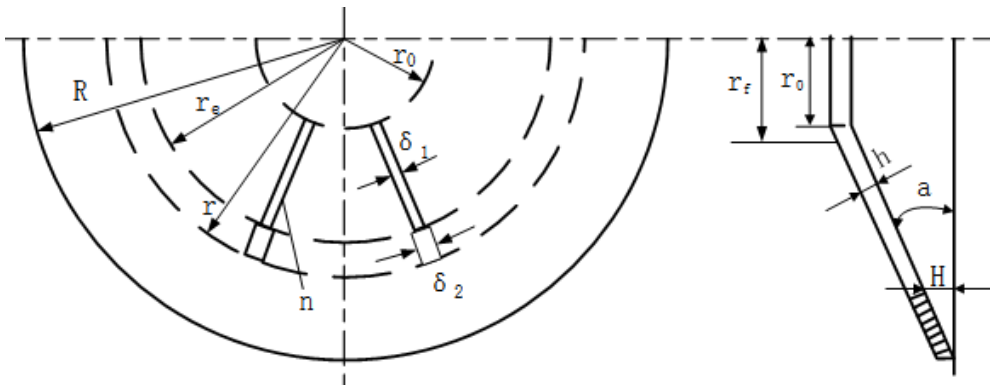

(b) Square window hole

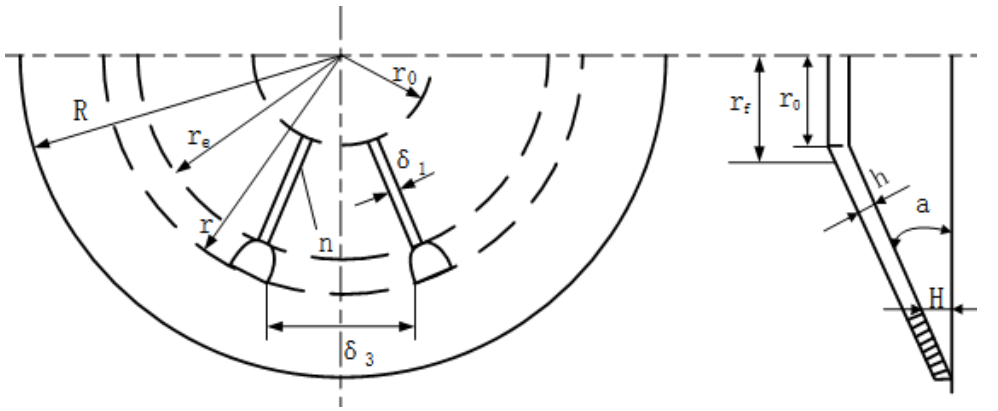

(c) Trapezoidal window hole

Fig.1. Diaphragm spring structure diagram of three different window holes

2.1. Determination of H/h and h

The characteristic curve of the diaphragm spring elasticity is shown in Fig. 2. The characteristics of the diaphragm spring are related to the ratio of the taper height H of the original inner section to the thickness h of the spring diaphragm, which has a great influence on the elastic properties of the diaphragm spring [10]. Different H/h ratios can give different denaturation characteristics. When $H/h < \sqrt{2}$, the shape of its characteristic curve shows the nature of the incremental function. As the load increases, the deformation increases continuously, indicating that the diaphragm spring has a large rigidity, withstands a large load, and is suitable for the stroke limiter of the buffer device. When $H/h = \sqrt{2}$, the elasticity has a flat curve in the middle section, and the external load corresponds to the extreme point in the function at this time. This point is exactly the inflection point, and the load is basically unchanged as the deformation increases [11]. This spring thus becomes a zero-stiffness spring. When $\sqrt{2} < H/h < 2\sqrt{2}$, the spring characteristic curve has a negative stiffness region, that is, the load reduces under the positive value of deformation. This feature is suitable for the clutch spring. The clutch of this characteristic diaphragm spring can use its negative stiffness

region to reduce the load when the clutch is disengaged [12]. When $H/h \geq 2\sqrt{2}$, this characteristic spring is suitable for the locking mechanism in the hydraulic drive of automobiles due to the load-bearing area.

Generally, the H/h of all diaphragm springs of the automobile clutches is usually selected between1.5-2 to ensure small pressure changes and easy operation [12]. In this design, the parameters are $H/h = 1.8$, $h = 1.8mm$, and $H = 3.24mm$.

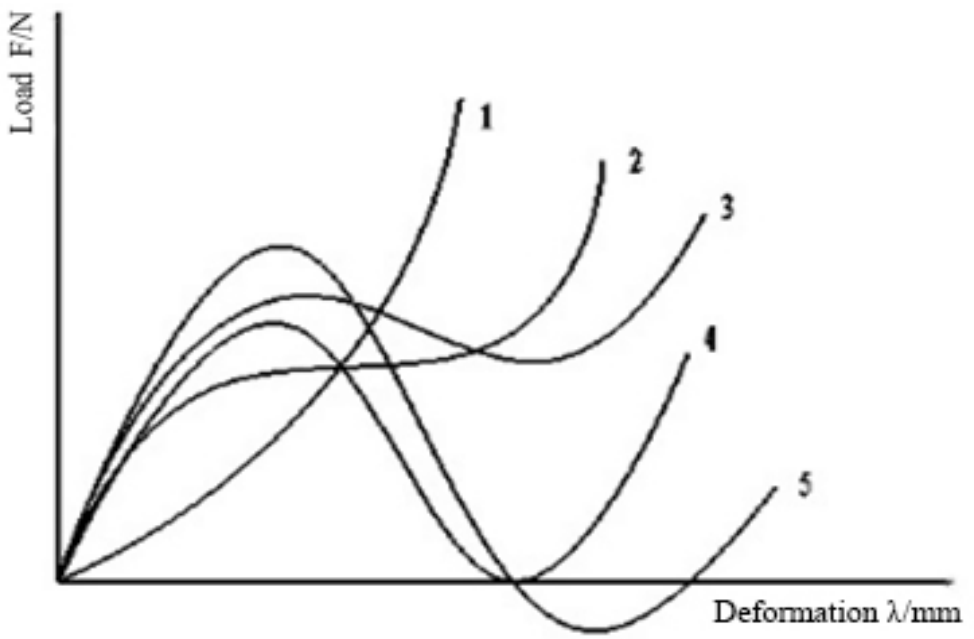

1) $H/h < \sqrt{2}$
2) $H/h = \sqrt{2}$
3) $\sqrt{2} < H/h < 2\sqrt{2}$
4) $H/h = 2\sqrt{2}$
5) $H/h > 2\sqrt{2}$

Fig.2. The elastic characteristic curve of the diaphragm spring

2.2. Selection of R/r and r

The popular diaphragm clutches on the market are divided into push-pull types. The push - pull classification is based on the nature of the force applied to the spring release pointing end face when the clutch is disengaged in operation, regardless of whether it is under tension or pressure. The diaphragm structure of the push-pull clutches is opposite to the push-pull diaphragm spring clutch. Pull-type clutch is a new structure [11], which has the advantages of small axial dimensions, light overall mass, simple structure, easy disassembly and installation, good heat dissipation and low operating force requirement. Under the same external operation, the pull-type diaphragm spring clutch requires fewer clutch force [6]. In this design, all references to the tension diaphragm spring clutches refer to the pull-type diaphragm spring clutches.

To evenly distribute the stress on the friction plate, the r-value of the pull-type diaphragm spring is greater than or equal to the average radius R_c of the clutch friction plate.

To make the stress on the friction plate evenly distributed, when the r-value of the pull-type diaphragm spring is greater than or equal to the average radius of the clutch friction plate RC, the friction plate pressure distributes uniformly, and RC is calculated according to the formula,

$$R_c = \frac{1}{3} \cdot \frac{D^3 - d^3}{D^2 - d^2}$$

where

D - The outer diameter of the friction plate;

d - The inner diameter of the friction plate; and

c - The friction disc inner and outer diameter ratio.

When $\frac{R}{r} = 1.2 \sim 1.35$ [13] is ensured, $\frac{R}{r} = 1.3$, $r = 63.676mm$, and $R = 82.779mm$.

2.3. Use the appropriate taper angle α

The conical slope of the diaphragm spring at zero load should be limited to between 9° and 15° [13]. The relationship between the conical bottom angle α of the diaphragm spring and the height H of the inner truncated cone is as follows:

$$\alpha = arctan\frac{H}{R-r} \tag{1}$$

The known parameters can be α = 14 °, which meets the requirements.

2.4. Selection of the separation index n

The diaphragm spring separation of vehicles refers to the selection number r. The large-size diaphragm spring has 24 choices, and the small-size spring can use 12 [10]. The design separation refers to the number $n = 16$.

Observing the diaphragm springs with different window holes and considering that the influence of the separation finger part on the vibration deformation characteristics is concentrated on the root of the separation finger and the window hole structure, the separation finger structure of the diaphragm spring is transformed, and the transformed diaphragm spring is shown in Fig. 3.

2.5. Selection of the inner diameter o of the separation end and the radius of the loading point f of the separation device

The number of r_0 is determined by the installation structure, and its minimum is greater than the outer diameter of the slave shaft spline. In addition, $r_f > r_0$ [9] is required, and $r_0 = 24\ mm$ and $r_f = 26\ mm$ in this design.

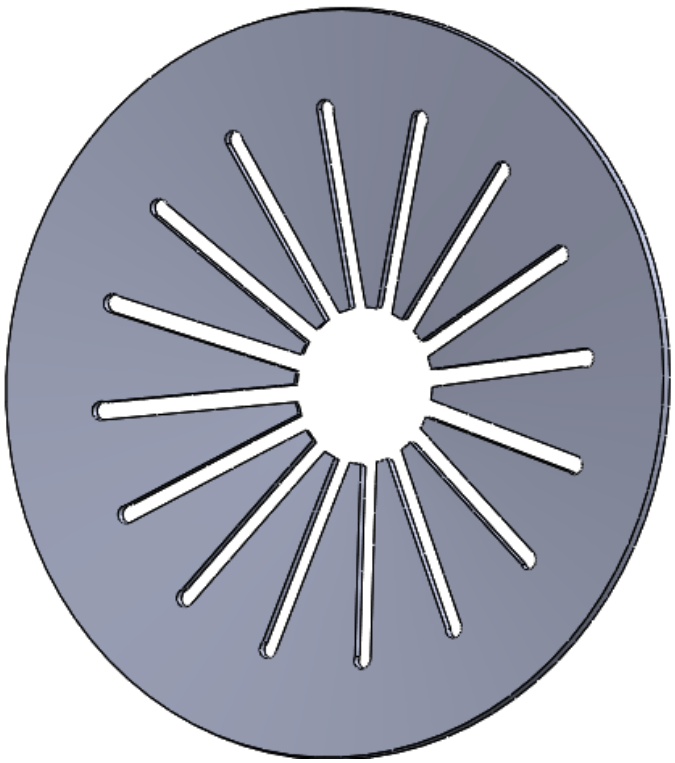

Fig. 3. The geometric model of the transformed diaphragm spring

2.6. Determination of the groove width δ_1, δ_2 and radius r_e

Usually, the slot width of diaphragm spring should be in the range of δ_1= 3.2-3.5mm, δ_2= 9-10mm, and the value of r_e should meet the requirement of [10]:

$$r - r_e \geq \delta_2 \tag{2}$$

where δ_1 = 3.3mm, δ_2 = 9.5mm, and r_e = 50mm.

2.7. Selection of the action radius R_1 of the clutch cover loading point and the action radius r_1 of the pressure plate support point

The stiffness of the diaphragm spring is affected by the applied loading radius. Based on the diaphragm structure distribution, the corresponding loading radius approaches the inner and outer radius of the spring [6]. R_1=77.6mm and r_1=66.5mm.

Generally, the parameters of the diaphragm spring clutch in this design are shown in Table 1.

Table 1. The values of diaphragm spring parameters

Parameters	Values
$H\ /mm$	3.24
$h\ /mm$	1.8
$R\ /mm$	82.779
$r\ /mm$	63.676
R_1/mm	77.6
r_1/mm	66.5
δ_1/mm	3.3
δ_2/mm	9.5
r_e/mm	50
r_0/mm	24
r_f/mm	26
n	16

3. OPTIMAL DESIGN OF THE DIAPHRAGM SPRING

3.1. Optimal design variables for the diaphragm spring

The final results of the optimized design are to determine the size parameters of a set of diaphragm springs to meet the requirements of performance. It can be seen from the load-deformation relationship of the diaphragm spring: The main independent parameters that affecting the diaphragm spring are H, h, R, r, R_1, and r_1 [11]. Among them, the thickness h of the diaphragm spring affects the extreme pressure of the clutch. The outer radius R of the diaphragm spring would affect the stress characteristics of the diaphragm spring. The high taper H will affect the axial deformation of the large end of the clutch diaphragm under the minimum load. The performance of the diaphragm spring would be affected by the above six variables, and the expression of the variable parameters for optimal design is $X = [H, h, R, r, R_1, r_1]^T$.

3.2. Checking the stress calculation of the diaphragm spring

As shown in Fig. 4, if the spring rotates rigidly at a zero-stress point O on the section plane, the cross-section point O would rotate one circle around the center of the diaphragm spring to form a zero tangential stress surface. Under no-load, the X-axis is established through the point O and the cone angle of the horizontal spring pointing to the bottom of the cone. The stress value at any point on the section plane is:

$$\sigma_t = \frac{E}{1-\mu^2} \cdot \frac{x\phi(\alpha-\phi/2)-y\phi}{e+x} \tag{3}$$

where α is the cone angle of the diaphragm spring under zero load; ϕ is the meridian corner from the free state; e is the zero-stress layer coordinate origin radius; μ is the Poisson ratio, and E is the elastic modulus.

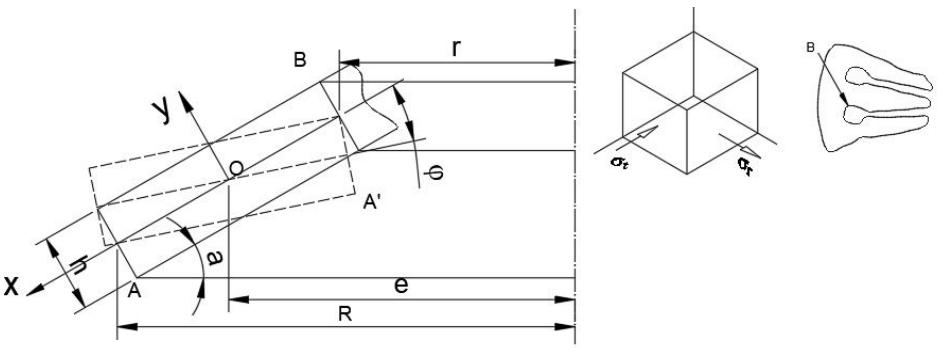

Fig. 4. Stress of the diaphragm spring - by trying

The stress distribution on the section can be explained conveniently, and the relationship between X and Y can be derived from equation (3):

$$Y = \left[\left(\alpha - \frac{\phi}{2}\right) + \frac{(1-\mu^2)\,\sigma_t}{E\,\phi}\right] X + \frac{(1-\mu^2)\,\sigma_t\, e}{E\,\phi} \tag{4}$$

The expression clearly shows that when the turning angle ϕ of the meridian section is a certain value, the X-Y of the tangential stress σ_t satisfies the characteristics of a linear function.

On the zero-stress layer, $Y = (\alpha - \frac{\phi}{2})X$ and $(\alpha - \frac{\phi}{2})$ are negligible again. At this moment, let $tan(\alpha - \frac{\phi}{2}) = (\alpha - \frac{\phi}{2})$, there is $Y = tan(\alpha - \frac{\phi}{2})X$. It shows that the plane on the straight line passing through the origin and forming $(\alpha - \frac{\phi}{2})$ with the horizontal axis is the zero-stress plane. From formula (4), it is found that when $X = -e$, Y remains unchanged, i.e., $Y = -(\alpha - \frac{\phi}{2})e$. That is to say, for certain ϕ, the iso-stress lines all converge on the point K (as shown in Figs. 5 and 6). That is, the line passing through K and O is the node; the area below K and O is the compressive stress area, and the above is the tensile stress. If the stress is far away from KO, its value will become larger [12]. The maximum compressive stress appears at B, and the tensile stress appears at A.

To ensure that the tangential stress at B reaches the maximum without damage, $X = -(e - r)/\cos\alpha \approx -(e - r)$ and $Y = \frac{h}{2}$ are substituted into equation (4) to obtain:

$$\sigma_{tB} = \frac{E}{(1-\mu^2)\,r} \cdot \left\{\frac{e-r}{2}\phi^2 - \left[(e-r)\alpha + \frac{h}{2}\right] \cdot \phi\right\} \tag{5}$$

The stress and the rotation angle are differentiated on both sides to set $\frac{d\sigma_{tB}}{d\phi} = 0$, it is found that the rotation angle is $\phi = \alpha + \frac{h}{2(e-r)}$, where the tangential compressive stress reaches the maximum value.

From the above derivation, it can be known that the maximum compressive stress of point B appears when the position of the spring butterfly part is sub-flattened by an angle $\frac{h}{2(e-r)}$. This situation is only possible when it is separated, and it does not mean that there is $\phi = \alpha + \frac{h}{2(e-r)}$ in all cases. When the clutch is completely disengaged, the meridian section of the diaphragm spring is actually larger than $\frac{h}{2(e-r)}$. Point B is a certain point of the root of the separation finger, and its bending stress under the axial load P_2 is:

$$\sigma_{rB} = \frac{M}{W_n} = \frac{(r-r_f)P_2}{n\frac{\delta_2 h^2}{6}} = \frac{6(r-r_f)P_2}{n\,\delta_2\,h^2} \tag{6}$$

Taking into account the influence of stress concentration on stress, the width coefficient of the root of the separation finger is introduced to the formula (6):

$$\beta = 1 - \frac{\delta_2\, n}{\pi(r_e+r)} \tag{7}$$

where $\delta_2$is the width of the root of the separating finger; n is the number of separated fingers, and $r_e$is the separation refers to the radius of the front widest part.

The above equation is substituted into equation (6) to achieve the stress of the diaphragm spring, σ_{tB}=1621.8 and σ_{rB}=570.795. According to the theory of maximum shear stress strength, combined with the formula A-L, the equivalent stress and strength requirements of point B can be derived as:

$$\sigma_{VB} = \frac{E}{1-\mu^2}\cdot\frac{\lambda}{R_1-r_1}\left[\left(\frac{R-r}{r\,ln\frac{R}{r}}-1\right)\left(\frac{H}{R-r}-\frac{\lambda}{2(R_1-r_1)}\right)+\frac{h}{2r}\right]-\frac{6P_2(r-r_f)E}{\pi r\beta h^2} \tag{8}$$

$$\sigma_{VB} \le [\sigma_{VB}] = 1700N/mm^2 \tag{9}$$

The two stress values are substituted into formula (8) to obtain σ_{VB}=1051N/mm^2. The above stress meets the requirements [13], and the data is appropriate.

3.3. The objective function for diaphragm spring optimization

According to the main functions of the clutch, it is required to optimize the structure and reduce the separation force of the clutch separation system to the operator under the normal operation. If the minimum separation force only needs the clutch diaphragm spring, the load-deformation curve will become steeper [14]. On the other hand, the average change of the diaphragm spring working pressure is the smallest, which will inevitably flatten the load-deformation curve. Multi-objective optimization is thus carried out.

To ensure that the clutch can transmit the torque of the engine, the system overload is avoided, and the separation force of the operating system is required to be reduced. The clutch

in the Life Cycle of Friction Plate is chosen [15]. The first objective function is to minimize the absolute value of the average change of the pressure on the diaphragm spring relative to the initial working point, that is:

$$\begin{cases} f_1(x) = \mathrm{Min}\dfrac{1}{5}\displaystyle\sum_{i=1}^{5}\left|P_1\left(x_1, x_2, x_3, x_4, x_5, x_6, x_7 - \dfrac{i}{5}\Delta\lambda\right) - P_1(x_1, x_2, x_3, x_4, x_5, x_6, x_7)\right| \\ x = [x_1, x_2, x_3, x_4, x_5, x_6, x_7]^T = [H, h, R, r, R_1, r_1, \lambda]^T \end{cases} \tag{10}$$

When the clutch friction disc reaches its life cycle, the torque can be reliably transmitted after wear of the clutch friction disc. Considering that the friction coefficient will decrease with wear [14], as the second objective function, the pressure range of diaphragm spring is small after the wear of the clutch friction disc, that is:

$$\begin{cases} f_2(x) = \mathrm{Min}P_1\left(x_1, x_2, x_3, x_4, x_5, x_6, x_7 - \lambda_f\right) - P_1(x_1, x_2, x_3, x_4, x_5, x_6, x_7) \\ x = [x_1, x_2, x_3, x_4, x_5, x_6, x_7]^T = [H, h, R, r, R_1, r_1, \lambda]^T \end{cases} \tag{11}$$

where, $\lambda_f$is the travel of the clutch platen, generally with $1.8\sim2.2mm$;$x_7(\lambda)$ is the axial displacement of the diaphragm spring, with $2.625mm$;

The above two objective functions are transformed into single objective functions by weighting method, ω_1=0.7 and ω_2=0.3. The objective function of the optimal design is:

$$\begin{cases} F(x) = \omega_1 f_1(x) + \omega_2 f_2(x) \\ x = [x_1, x_2, x_3, x_4, x_5, x_6, x_7]^T = [H, h, R, r, R_1, r_1, \lambda]^T \end{cases} \tag{12}$$

3.4. Constraint conditions for optimum design of diaphragm springs

The H/h ratio of diaphragm spring height to thickness has a great influence on the load-deformation characteristic curve, and its ratio should conform to a certain range:

$$1.5 \le H/h \le 2 \tag{13}$$

The relative size ratio of each part of diaphragm spring should be taken in a certain range.

$$\begin{gathered} 1.20 \le R/r \le 1.35 \\ 70 \le 2R/h \le 100 \\ 3.2 \le R/r_0 \le 5.0 \end{gathered} \tag{14}$$

To evenly distribute the pressing force on the clutch friction plate, the radius R_1 of the loading point of the pressure plate of the pull-type diaphragm spring should be between the radius of the friction disc and the outer diameter of the friction disc [9]:

$$\frac{D+d}{4} \le R_1 \le \frac{D}{2} \tag{15}$$

When the diaphragm spring is in Free State, the service of the clutch diaphragm spring should be satisfied. The initial cone bottom angle α of the diaphragm spring is within a certain range. The relation between the cone bottom angle a of the diaphragm spring and the height h of the intersection cone [9]:

$$9° \leq \alpha = arctan\frac{H}{R-r} \leq 15° \tag{16}$$

According to the Layout Requirements, the difference between R_1 and R, r and r_1, r_f and r_0 should be within a certain range:

$$\begin{aligned} 1 \leq R - R_1 \leq 7 \\ 0 \leq r_1 - r \leq 6 \\ 0 \leq r_f - r_0 \leq 4 \end{aligned} \tag{17}$$

When the clutch works, the diaphragm spring replaces the compression spring, and the separation finger acts as a separation lever [6]. The leverage ratio should be selected within a certain range:

$$3.5 \leq \frac{r_1 - r_f}{R_1 - r_1} \leq 9.0 \tag{18}$$

3.5. Mathematical model for optimal design of the diaphragm spring parameters

For the diaphragm spring of the pull-type diaphragm spring clutch, the optimized mathematical model (forming the mathematical model form of the standard optimization algorithm) is [15]:

$$MinF(x) = \omega_1 f_1(x) + \omega_2 f_2(x)$$

St.

1) $H - 2h \leq 0$
2) $1.5h - H \leq 0$
3) $R - 1.35r \leq 0$
4) $1.2r - R \leq 0$
5) $2R - 100h \leq 0$
6) $70h - 2R \leq 0$
7) $R \div 24 - 5 \leq 0$
8) $3.2 - R \div 24 \leq 0$
9) $(9)R_1 - 80 \leq 0$
10) $67.5 - R_1 \leq 0$
11) $H - (R - r) \cdot tan\left(\frac{15\pi}{180}\right) \leq 0$

12) $(R-r)\cdot tan\left(\frac{9\pi}{180}\right)-H\leq 0$
13) $R-R_1-7\leq 0$
14) $1+R_1-R\leq 0$
15) $r_1-r-6\leq 0$
16) $r-r_1\leq 0$
17) $(r_1-26)-9(R_1-r_1)\leq 0$
18) $3.5(R_1-r_1)-(r_1-26)\leq 0$

4. ANALYSIS OF DIAPHRAGM SPRING PARAMETER OPTIMIZATION DESIGN RESULTS BASED ON GENETIC ALGORITHM

Genetic algorithm is an optimization algorithm developed by simulating and analyzing the genetic characteristics of natural organisms and the evolution mechanism of organisms. Its calculation efficiency has gradually increased with more practicality and strong robustness.

Many intricate factors need to be considered in the optimization design of clutches. These intersecting factors, to a certain extent, indicate the multidimensionality of the clutch in optimal design, that is, the non-uniqueness of the target decision variables. Considering the overall planning of the genetic algorithm, it is used to optimize the design of the clutch and simply the problems. In various complex constraint systems, traditional optimization models that approximate to the global optimal solution are used to deal with the analysis problem [16]. As well known, the typical characteristics of the genetic algorithms are [16] that it does not require auxiliary information for group search but use an inherent heuristic random search method. It also has the characteristics of global optimization and is not easy to fall into local optimization, so that it is more suitable for solving complex problems. Combined with the characteristics of genetic algorithm optimization of survival of the fittest design decision variables, and the powerful processing functions of MATLAB software, this paper adopts a combination of the two for clutch optimization. The genetic algorithm based on MATLAB is used to optimize the structure of the clutch, which can realize the human-computer interaction analysis and processing mode at the same time.

4.1. The genetic algorithm flow

The genetic algorithm uses three operators: selection, crossover and mutation, to start from any initial population of the population. According to the specific probability and corresponding conditions, a new group of individuals that can adapt to the environment are generated. Repeated iterations in this way can eventually converge to the individuals with the strongest environmental adaptation, that is, the global optimal solution. The specific strategy model is shown in Figure 4. For example, for a general optimization problem of function maximization or minimization, it is equivalent to solving a constrained mathematical model:

Max F(X)
s.t. X∈R
R∈U
Among them, X=[x1,x2…xn] is the decision variable of the function
f(X) is the objective function
R feasible solution set

U basic space
The basic genetic algorithm mathematical model:
SEA = (C, E, P0, M, SEL, MUT, XOV, T)
Among them, C—individual coding method
E—Individual fitness evaluation function
P0—initial population
M—population size
SEL—selection operator
MUT—mutation operator
XOV—crossover operator
T—termination condition (genetic evolution algebra)

Scholars from the University of Sheffield developed a tool function for the genetic algorithm based on the MATLAB high-level language. Due to the versatility of MATLAB language, the genetic algorithms are highly compatible with data analysis, visualization tools, and special application fields of the language [17]. The search tool can be accessed directly through the command line and graphical user interface of MATLAB software. At the same time, the graphical analysis and operation results of the monitoring and output results can also be visualized through the command line and graphical user interface of MATLAB.

The main steps are as follows:

1) Encode according to the parameter set of the problem to be solved;
2) Initialize the group;
3) Calculate the fitness value of each individual in the group;
4) Select individuals who will enter the next generation according to a certain rule determined by the fitness value of the individual;
5) Carry out crossover operations according to crossover probability;
6) Carry out mutation operations according to mutation probability;
7) Generate new individuals;
8) If a certain termination condition is not met, return to step (3), otherwise go to step (9);
9) Output the population with the best fitness value in the population as the satisfactory solution or optimal solution of the problem.

4.2. Operators of genetic algorithm variation

1) Based on the previous generation of individuals, three genetic operators of selection, crossover and mutation acting on the population composed of M individuals will produce a new generation of groups with higher fitness function values, that is, M design points with more and more accurate objective function values meeting the constraints. Selection operation uses local competitive selection operator; crossover operations use single-point crossover operators, and mutation operations use basic bit mutation operators.
2) The fitness function value based on the individual is selected for the individual to be copied to the next generation. The selection uses a proportional operator, that is, the

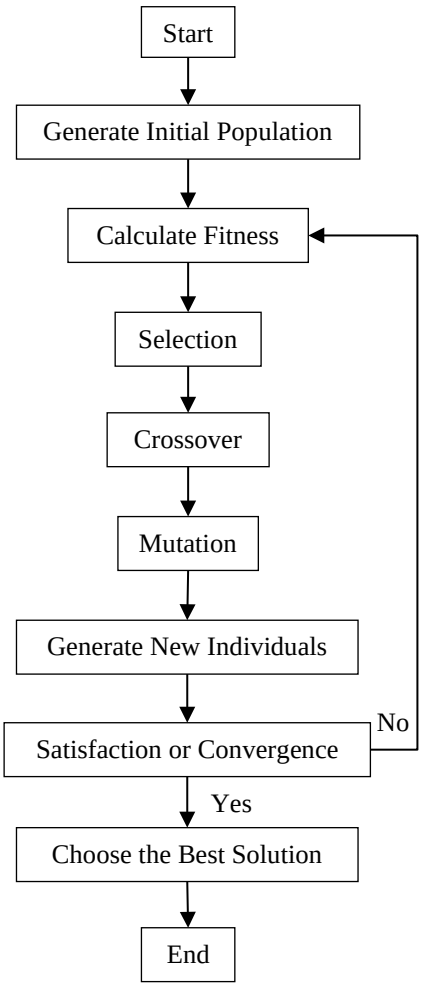

Fig. 5. Program design flow chart

probability that an individual is selected and inherited into the next generation is proportional to the fitness of the individual. The probability of each individual being selected is the proportion of its fitness in the fitness of the group.

3) The crossover is to randomly select two individuals as the parent body, and then randomly exchange the subsequent substrings at a certain position in the parent body to form two new individuals. The crossover uses the uniform crossover operator, that is, the genes on each locus of the two paired individuals are exchanged with the same crossover probability, forming two new individuals.

The mutation refers to randomly replacing some gene values in the individual code with other alleles with a small mutation probability, thereby forming two new individuals. The mutation uses the basic position operator, i.e., randomly assigning the mutation probability to change the gene value of a certain position or a certain gene seat in an individual, making it an allele of other genes.

4.3. Optimum design process of diaphragm spring parameters

The characteristics of the objective function involved in this design are multivariable and single peak [18]. The genetic algebra $T = 10$ and population size $M = 100$ are set in the genetic algorithm. The selection principle adopts roulette gambling strategy, and the crossover principle uses scattered intersection. The crossover probability is $P_c = 0.8$; the mutation probability is $P_m = 0.01$, and the fitness function selects the objective function after linear weighting [19-20].

In this optimization, the value of the objective function is returned by $c(x)$ and $ceq(x)$. lb and ub are the lower and upper bounds of the variables, respectively [21]. According to the expression of the objective function, a function M file named Yichuan m, and a constraint M file of the function named CSXunconYan m file, are written to save in the MATLAB working file,lb = [3.5,2,80,55,76,56] and ub = [6,4,162.5,95,160,90].

4.4. Results of the new method for optimization design

The parameters are set in MATLAB, and then the Start button is clicked to start the genetic algorithm. The results and process are as follows:

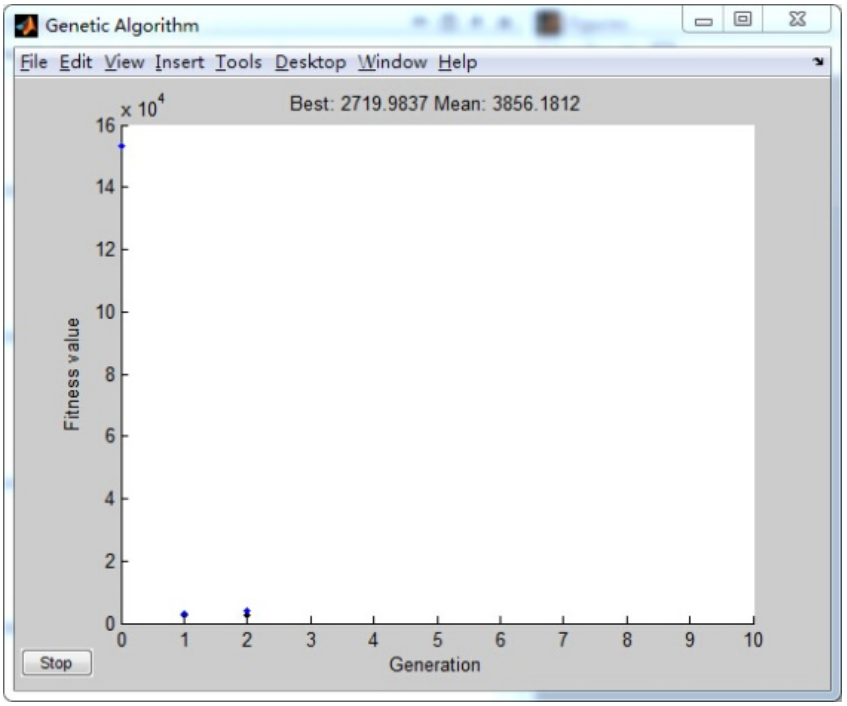

Fig.6. Individual fitness value of genetic second generation

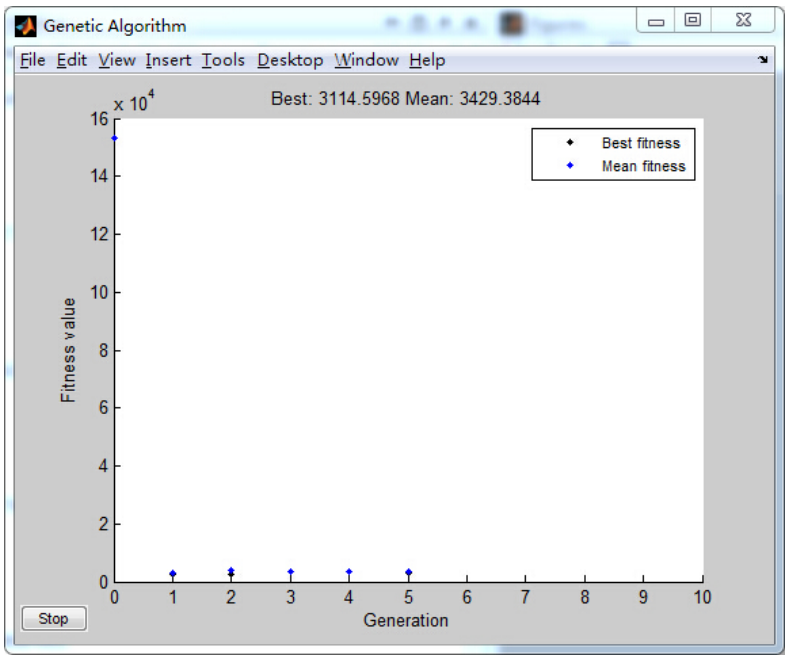

Fig. 7. Individual fitness value of genetic fifth generation

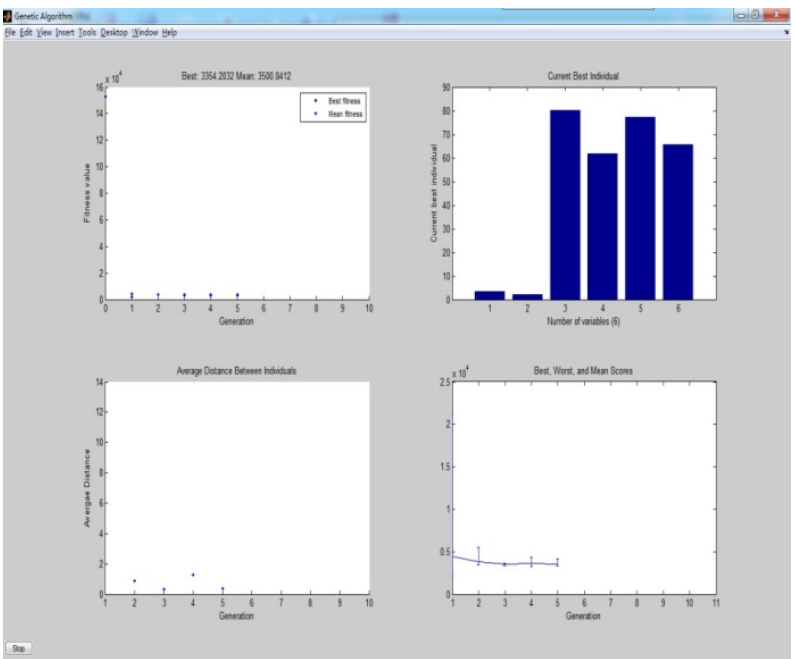

Fig.8. The objective function of optimal individual and individual distance, based on the rank of fitness best, worst and average score with the change of genetic algebra

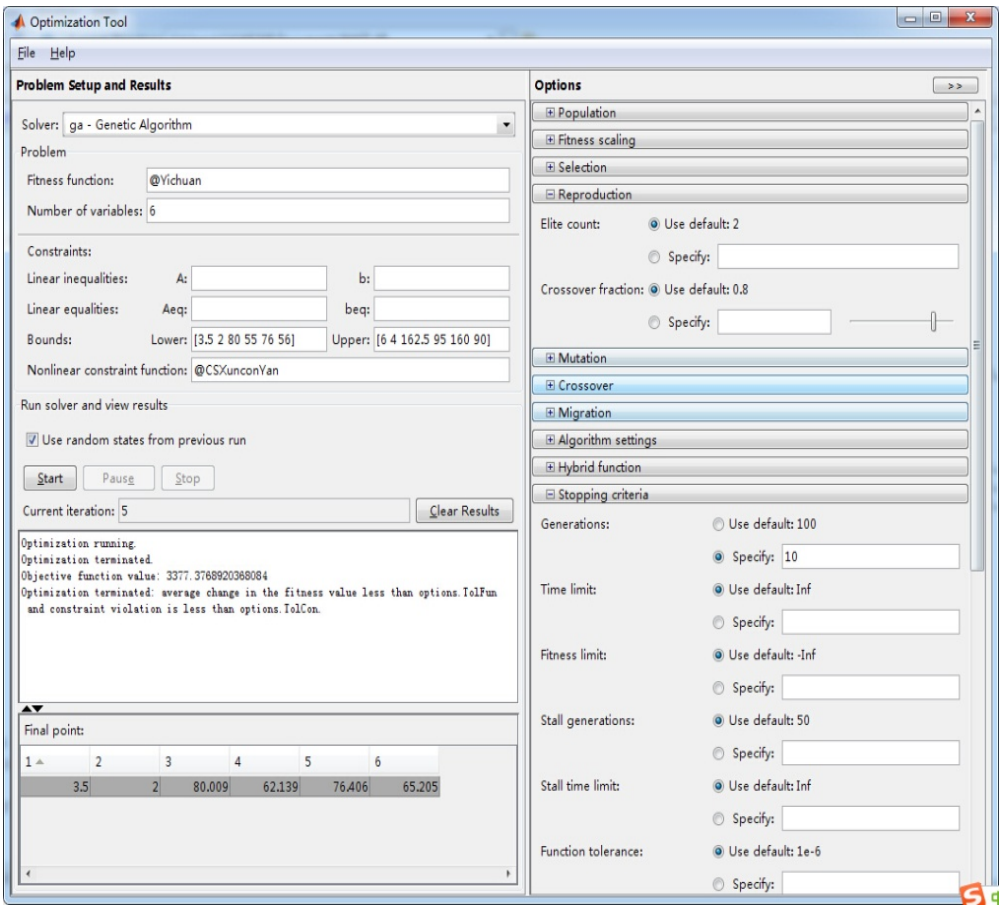

Fig.9. Genetic algorithm toolbox of parameter setting and optimization results

It can be seen from Fig.9 that the final result of this optimization is $X = [H, h, R, r, R_1, r_1\ ]^T = [3.5, 2, 80.009, 62.139, 76.406, 65.205]^T$. To facilitate the comparison of optimized results [22], the parameters before and after optimization are compared, as shown in Table 2.

Table 2. Comparison of parameters before and after optimization design

Parameters	Pre-optimal design (original design)	After optimization design
H/mm	3.24	3.5
h/mm	1.8	2
R/mm	82.779	80.009
r/mm	63.676	62.139
R_1/mm	77.6	76.406
r_1/mm	66.5	65.205

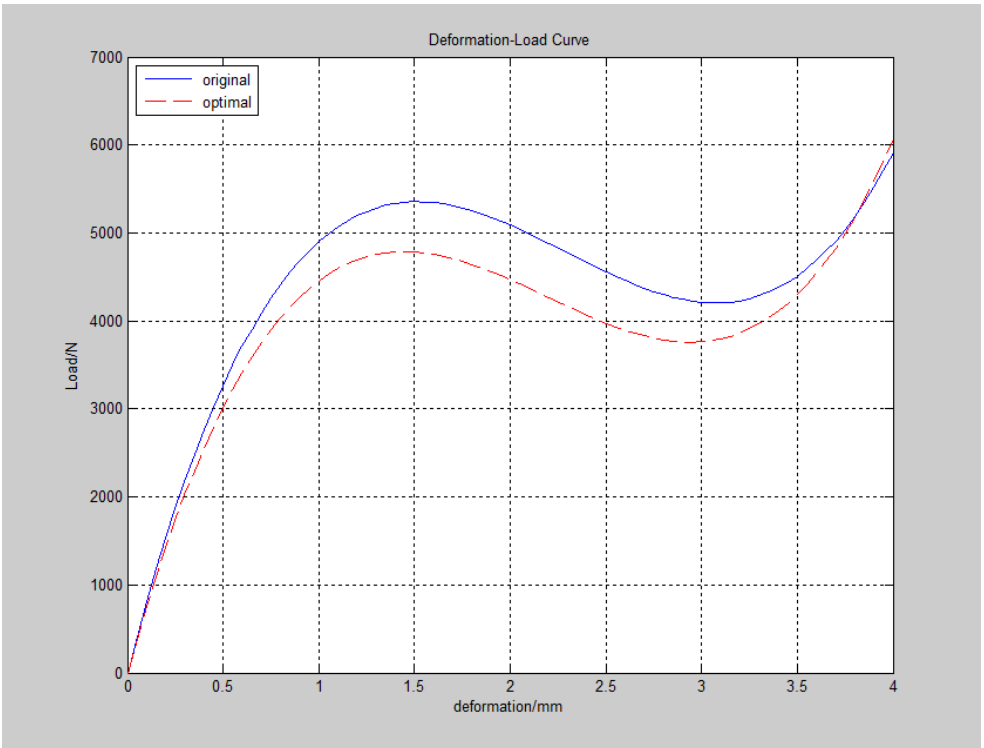

Fig.10. Comparison of load-displacement characteristic curves of diaphragm springs after and before genetic optimization of algorithms

As shown in Fig.10, the optimized line in the first half is more moderate than the original design, indicating that the mean value of the compression force of the diaphragm spring decreases during the wear of the clutch friction plate, so that the backup coefficient of the clutch is more stable than the original design. The latter half is also gentler than the original design function image, indicating that the optimized clutch separation force changes little, making the separation and handling performance more stable than the original design [23-26]. The performance of optimized diaphragm spring is better than that before optimization, indicating the proposed method is feasible and effective.

5. EXPERIMENTAL COMPARISON OF VIBRATION CHARACTERISTICS OF DIAPHRAGM SPRINGS

5.1. Finite element analysis method for diaphragm springs

From the equivalent stress clouds with axial displacements of 3 mm, 6 mm, and 9 mm respectively (Fig.11), it can be seen that the stress changes in the diaphragm spring during loading are mainly concentrated in the disc spring part and the window hole structure at the root of the separation finger. The equilibrium differential equation (19) in the elastic mechanic of the space problems establishes the relationship between the stress and body force [27-28].

$$\left.\begin{aligned}\frac{\partial \sigma_x}{\partial x}+\frac{\partial \tau_{yx}}{\partial y}+\frac{\partial \tau_{zx}}{\partial z}+f_x=0\\ \frac{\partial \sigma_y}{\partial y}+\frac{\partial \tau_{zy}}{\partial z}+\frac{\partial \tau_{xy}}{\partial x}+f_y=0\\ \frac{\partial \sigma_z}{\partial z}+\frac{\partial \tau_{xz}}{\partial x}+\frac{\partial \tau_{yz}}{\partial y}+f_z=0\end{aligned}\right\} \tag{19}$$

For diaphragm spring, it is necessary to balance the change of stress at the root of the separation finger and in the hole structure through the load, other than the load corresponding to the stress change of the disc spring part, that is, the bottom of the separation finger and the hole structure affect the vibration characteristics of the diaphragm spring [29].

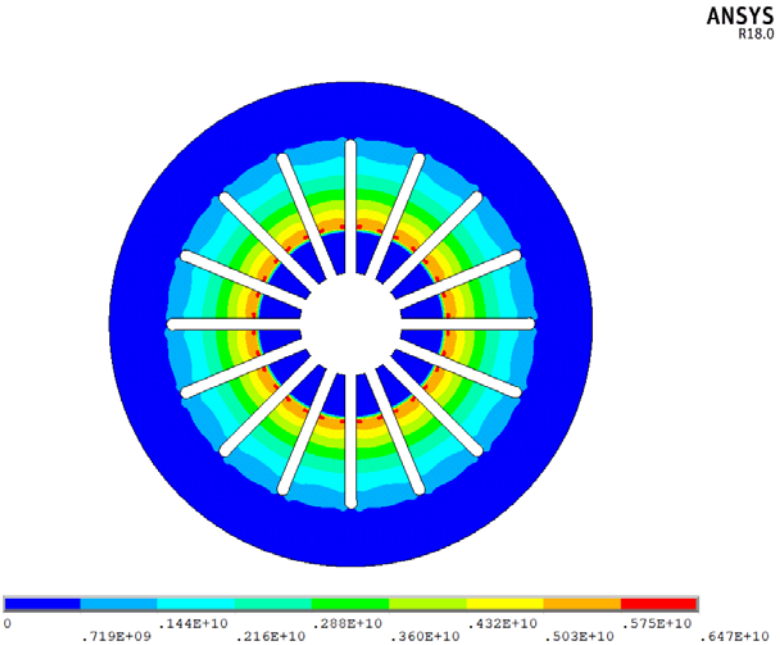

(a) Equivalent stress cloud for an axial displacement of 3mm

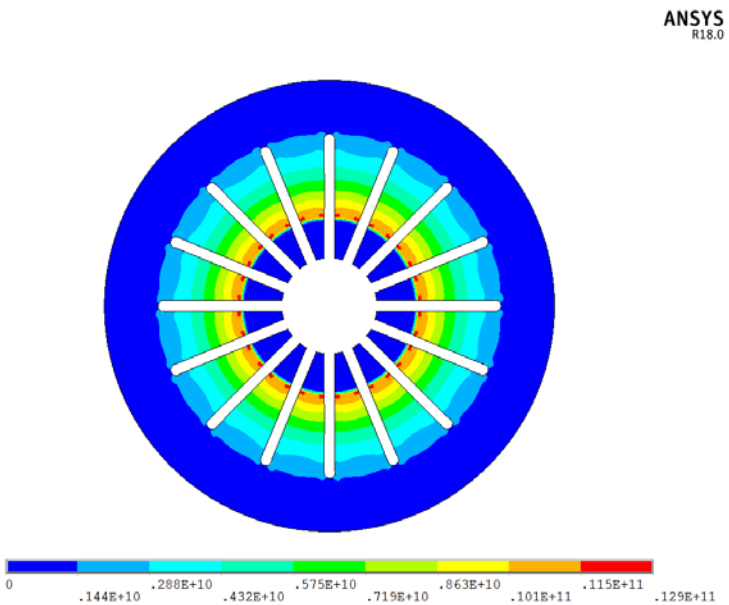

(b) Equivalent stress cloud for an axial displacement of 6 mm

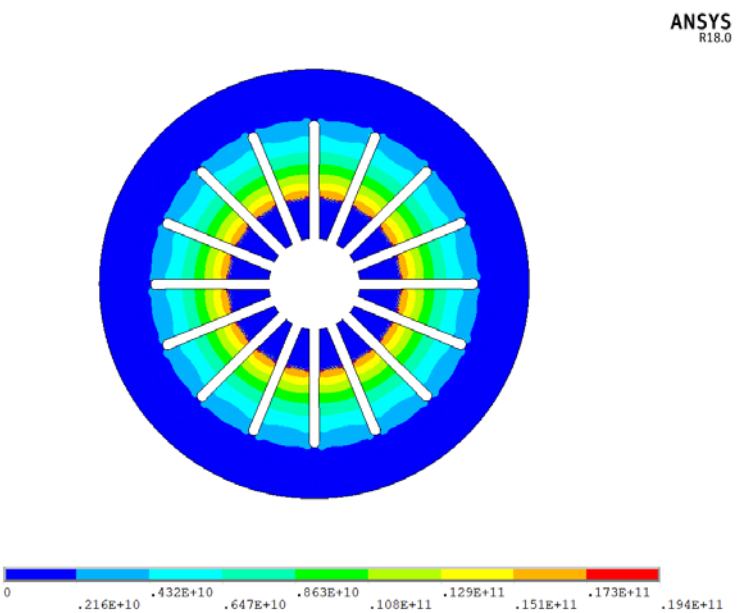

(c) Equivalent stress cloud for an axial displacement of 9 mm

Fig. 11. The equivalent stress cloud diagram with an axial displacement of 3mm, 6mm and 9mmrespectively

5.2. Measured data method

Three different window shapes of diaphragm springs, trapezoidal, square and oblong, are selected for verification in the test. 15 pieces are selected for each diaphragm spring (type A, type B and type C) to eliminate the influence of irregular shapes [30].

The convex side of the diaphragm spring is numbered (1-45) sequentially. The structural parameters of each diaphragm spring are measured by using vernier calipers and vernier angles for 5 to 6 times to record the data. The diaphragm spring is placed on the lower die positioning arbor of the diaphragm spring load characteristic testing machine. The press is manipulated to load and unload the diaphragm spring after the big-end deformation reaches a certain stroke [31]. After the diaphragm spring test is completed, the test data stored in the press is exported.

Effective pressure test data is compiled for type A, type B and type C diaphragm springs. Through adding the peak and valley load displacement of each type of diaphragm spring under loading and unloading, the load displacement values of peak and valley excluding the effect of friction on the supporting surface are obtained, as shown in Table 3.

Table 3. The load displacement of peak and valley point without the influence of friction

Model	Peak Point Force	Peak point disp.	Actual disp.	Valley Point Force	Valley disp.	Actual disp.
A	10303.7	-1.49	3.22	6893.6	1.09	5.60
B	10657.1	-1.50	3.17	6977.1	1.16	5.64
C	10496.3	-1.47	3.22	7050.0	1.15	5.62

5.3. Comparison verification

The load-deflection curves of the three types of membrane springs, type A, type B and type C, are calculated by the A-L method, the finite element method and the proposed method, respectively. The treated test curves are put into the same coordinate system for comparison, as shown in Fig. 12.

The peak and valley values of the three diaphragm springs calculated by the A-L method, the finite element method and the new method are compared with the measured values, as shown in Table 4. From Fig.12 and Table 4, it can be seen that the overall load-deflection curve of the A-L method is low, with low valley peaks and large errors, up to 13.2% and 18.65% respectively. The load-deformation curve of the finite element method is in good agreement with the measured curve before reaching the inflection point. After leaving the first inflection point, the load-deformation curve decreases fast, with a peak error of up to 1.42% and a valley error of up to 21.77%. The load curves of the new method are in overall better agreement and decrease after the first inflection point, but the decline is smaller, with a peak error of up to 1.89% and a valley error of up to 7.56%.

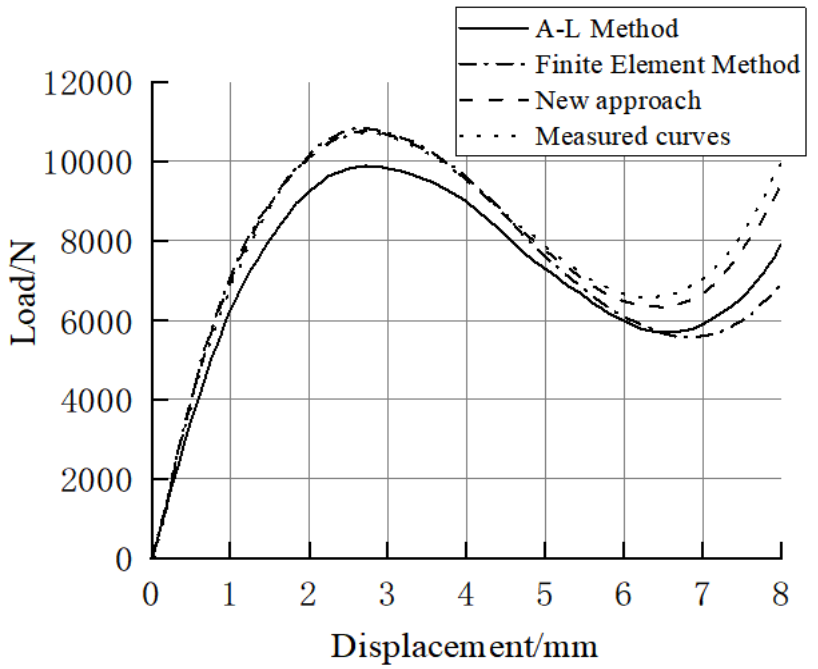

(A) Comparison of the calculation methods for the load characteristics of type A

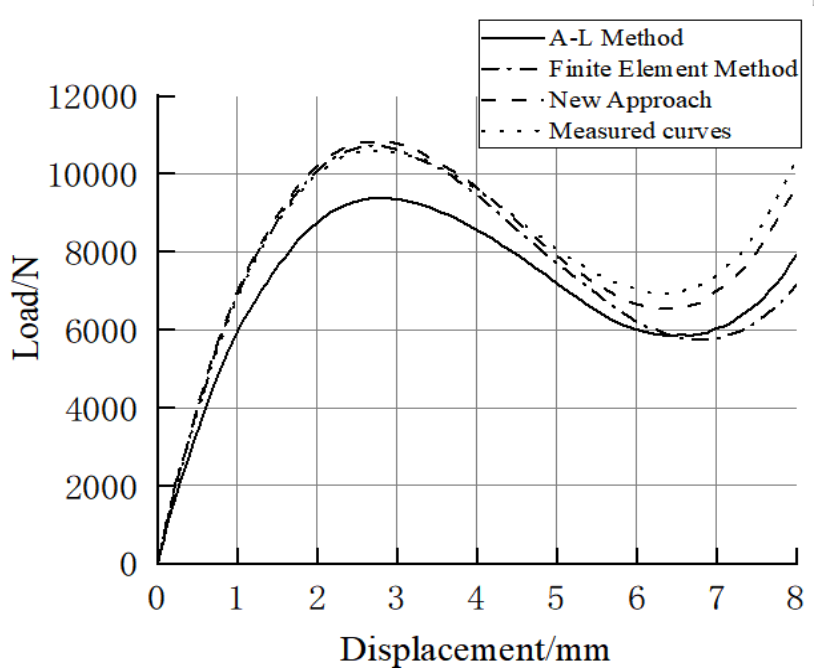

(B) Comparison of the calculation methods for the load characteristics of type B

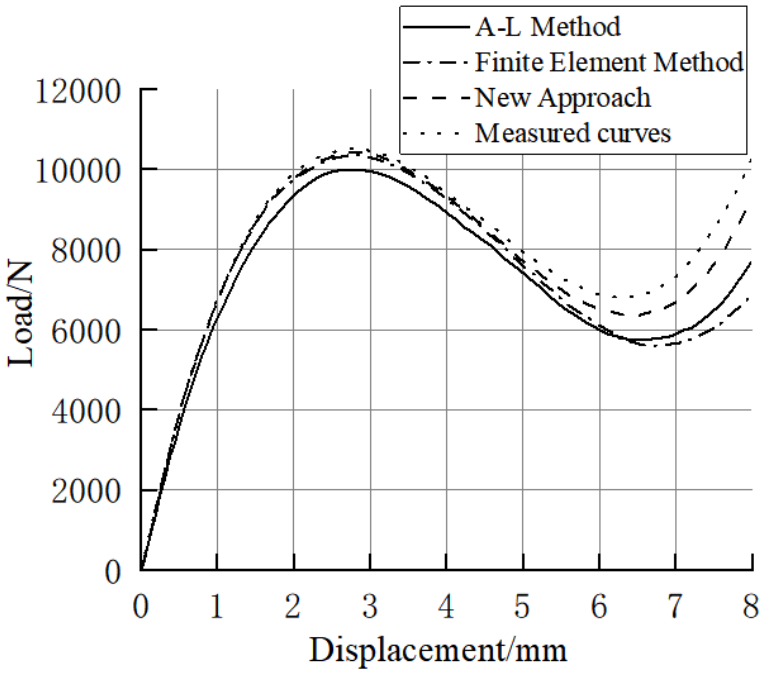

(C) Comparison of the calculation methods for the load characteristics of type C

Fig.12. Comparison of calculation methods for various load characteristics of three types of membrane springs

Table 4. Peak-to-valley point comparison of three methods

Model	Methods	Peak value	Valley Value	Peak relative error	Valley relative error
A	A-L method	9890.1	5701.4	-8.34%	-15.16%
	Finite Element Method	10844.2	5571.8	1.19%	-17.84%
	New Method	10787.7	6326.4	0.68%	-3.78%
	Actual measurement curve	10714.5	6565.8		
B	A-L method	9379	5849.4	-13.20%	-18.30%
	Finite Element Method	10727.3	5735.6	1.03%	-20.65%
	New Method	10821	6515.2	1.89%	-6.21%
	Actual measurement curve	10616.9	6920		
C	A-L method	9991.9	5741.9	-5.19%	-18.65%
	Finite Element Method	10363.4	5594.7	-1.42%	-21.77%
	New Method	10400.1	6334.2	-1.06%	-7.56%
	Actual measurement curve	10510.6	6812.8		

6. CONCLUSIONS

Considering the overall planning of genetic algorithm, it is used to optimize the clutch design and simplify the problem. In the complex constraint system with various faults, traditional optimization models that generate approximate global optimal solution is used to deal with the analysis problem. In addition, MATLAB software is used to optimize the parameters of diaphragm springs. The results of optimization show that it can greatly reduce the force of the clutch and meet the design requirements.

1) The objective function and mathematical model in the optimized design are feasible. Using this mathematical model to optimize the design of the diaphragm spring can achieve better results, and each decision variable of the optimized diaphragm spring is significantly better than the original design.
2) Genetic algorithm has better search ability than traditional optimization methods in multi-objective optimization and global optimization.
3) According to the test, the proposed method can control the peak error within 2% and the valley error within 8%. It can calculate the load-deformation characteristics of diaphragm springs with high accuracy and meet the requirements of engineering applications.

In the future, we will continue to study and improve the application of genetic algorithms in diaphragm spring parameters, as well as the application of other optimization algorithms in diaphragm springs and compare the application of different optimization algorithms in this field with genetic algorithms.

ACKNOWLEDGMENTS

Basic research business of undergraduate colleges and universities in Heilongjiang Province in 2020-General items (135509111); Heilongjiang Provincial Education Science "14th Five-Year Plan" 2021 Key Project (GJB1421342). Central guidance for local science and technology development special projects (SBZY2021E043). Education Science Research Project of Qiqihar University (GJQTYB202239). Qiqihar University Degree and Graduate Education Teaching Reform Research Project (JGXM_QUG_2020007).

REFERENCES

[1] Miu, Z.F., Pan, K.Q., Ma, H.Y., Analysis of Optimization of Automobile Clutch Diaphragm Spring. Science and Technology Innovation, 2018, (13): p. 150-151.
[2] Niknafs, H., Faridkhah, M., Kazemi, C., Analytical Approach to Product Reliability Estimation Based on Life Test Data for an Automotive Clutch System. Mechanics and Mechanical Engineering, 2018, 22(4): p. 845-863.
[3] Almen, J. O., & Laszlo, A., The uniform section disk spring. Transactions of the American Society of Mechanical Engineers, 1936, (58): p. 305-314.
[4] Yang, C., Finite element analysis of automobile clutch diaphragm spring (in Chinese). Mechanical & Electrical Technology, 2005, (1): p. 37-38.

[5] Yuan, D., Li, F., Zheng, F.C., Calculation for the load-deflection curve of diaphragm springs based on non-linear finite element method. Journal of Zhejiang University of Technology, 2009, 37(3): p. 350-354.

[6] Hu, R.K., Geng, L.D., Liu, F.Y., Correction Calculation Method for Load-Deformation Characteristics of Friction Clutch Diaphragm Spring. Machinery Design & Manufacture, 2021, (2): p. 169-173.

[7] Song, H.B., Lian, Z.M., Diaphragm spring optimization and simulation based on genetic algorithm toolbox. Journal of Yanbian University (Natural Science Edition), 2017, 43(1): p. 60-63.

[8] D'Angelo, G., Palmieri, F., GGA: A modified genetic algorithm with gradient-based local search for solving constrained optimization problems. Information Sciences, 2021, 547: p. 136–162.

[9] Musiałek, I., Migus, M., Olszak, A., Osowski, K., Kęsy, Z., Kęsy, A., Choi, S. B., Analysis of a combined clutch with an electro rheological fluid. Smart Materials and Structures, 2020, 29(8): p. 087006.

[10] Hiremath, N., Tarun, K. S., Static and modal analysis of diaphragm spring used in micro depth sensing indenting Machine. Materials Today: Proceedings, 2020, 20(Part 2): p. 161-166.

[11] Yan, Z.C., Wang, J.B., Optimal Design for Diaphragm Spring based on Modified Genetic Algorithm. Journal of Changzhou College of Information Technology, 2013, 12(1): p. 10-13.

[12] Cao, X., Du, C., Yan, F., He, B., Sui, Y., Parameter Optimization of Dual Clutch Transmission for an Axle-split Hybrid Electric Vehicle. IFAC-Papers online, 2019, 52(5): p. 423-430.

[13] Shangguan, W. B., Liu, X. L., Rakheja, S., Hou, Q., Effective utilizing axial nonlinear characteristics of diaphragm spring and waveform plate to enhance breakaway performances of a clutch. Mechanical Systems and Signal Processing, 2019, 125: p. 123-141.

[14] Song, D.B., Shan, Y., Jia, B.S., Study of Diaphragm Spring Clutch. Automobile Applied Technology, 2018, 44(11): p. 95-96.

[15] Ran, Z.Y., Zhao, S.E., Li, Y.L., Optimum Design for the Diaphragm Spring Clutch on Automobile with Genetic Algorithms. Journal of Chongqing University, 2003, (9): p. 77-81.

[16] Pährisch, M., Triebel, M., Sachs, Z.F., Influence of the manufacturing process on diaphragm springs for commercial vehicles and consideration thereof in the design phase. Drive System Technique, 2009, 23(2): p. 3-15+17.

[17] Majcherczak, D., Dufrénoy, P., Dynamic analysis of a disc brake under frictional and thermo mechanical internal loading. Archive of Applied Mechanics, 2006, 75: p. 497-512.

[18] Trotea, M., Constantinescu, A., Simniceanu, L., Analytical Calculation, Numerical Structural Analysis and Design Optimization of the Diaphragm Spring of a Mechanical Clutch. Applied Mechanics and Materials, 2020, 896: p. 151–162.

[19] Tang, H.L., Wang, J.B., Fuzzy Optimization Design of Diaphragm Spring Based on Genetic Algorithm. Mechanical Engineer, 2014, (9): p. 26-28.

[20] Zhang, W.B., Intelligent and optimal design for automobile diaphragm spring clutch. Chinese Journal of Construction Machinery, 2007, (1): p. 67-71.

[21] Shi, F.L., Summary of the development of mechanical structure optimization design. China Science and Technology Information, 2010, (22): p. 129+134.

[22] Huang, W.H., Optimization Design of Clutch Butterfly Compression Spring Based on Hybrid Genetic Simulated Annealing Algorithm. Journal of Mechanical Strength, 2009, 31(4): p. 675-677.

[23] Krishnasamy, K., Masse, F., Simon, O., Fatigue analysis of Diaphragm spring in double dry clutch including manufacturing process. Procedia Engineering, 2018,213: p. 606–612.

[24] Namvar, A. R., Vosoughi, A. R., Design optimization of moderately thick hexagonal honeycomb sandwich plate with modified multi-objective particle swarm optimization by genetic algorithm (MOPSOGA). Composite Structures, 2020, 252: p. 112626.

[25] Elhadidy, A. A., Elbeltagi, E. E., El-Badawy, S. M., Network-Based Optimization System for Pavement Maintenance Using a Probabilistic Simulation-Based Genetic Algorithm Approach. Journal of Transportation Engineering, Part B: Pavements, 2020, 146(4): p. 04020069.

[26] Chen, S.X., Cheng, X.W., Based on genetic algorithm optimal design on diaphragm spring by MATLAB. Machinery, 2016, 43(2): p. 48-52.

[27] Liao, S.Y., Yang, Y.C., Finite element analysis of the mechanical properties of diaphragm springs (in Chinese). Internal Combustion Engine & Parts, 2021, 329(05): p. 44-45.

[28] Jin, W.D., Finite Element Analysis of Diaphragm Spring for Automobile Clutch based on ANSYS Workbench. Journal of Mechanical Transmission, 2012, 36(05): p. 71-73+80.

[29] Ma, Y.J., Zhou, X., Optimization of Diaphragm Springs Based on Genetic Algorithm. Automobile Applied Technology, 2021, 46(07): p. 32-35.

[30] Shi, J.W., Wu, G.Q., Sensitive Factor of Diaphragm Spring Load Characteristics Analysis and Research Methods Contrast. Journal of Mechanical Transmission, 2013, 37(12): p. 113-118.

[31] Li, X., Yang, Y., Zhang, W., Wang, Z., Yuan, Y., Hu, H., & Xu, D., An FBG Pressure Sensor Based on Spring-Diaphragm Elastic Structure for Ultimate Pressure Detection. IEEE Sensors Journal, 2022, 22(3): p. 2213-2220.